Brief Communication

Cell Chemical Biology

Bacterial Alkaloid Biosynthesis: Structural Diversity via a Minimalistic Nonribosomal Peptide Synthetase

Graphical Abstract

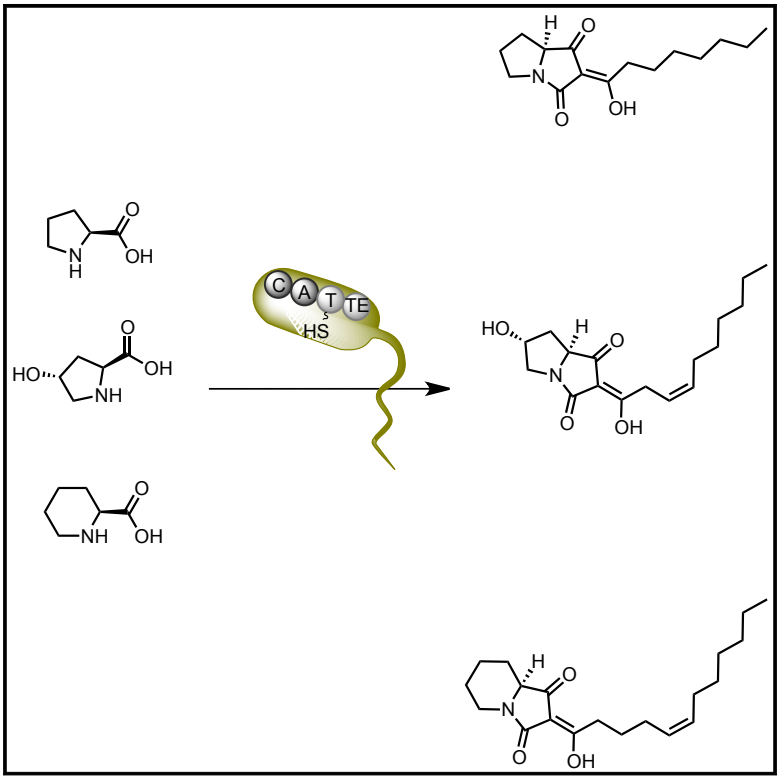

Authors

Martin Klapper, Daniel Braga, Gerald Lackner, Rosa Herbst, Pierre Stallforth

Correspondence

pierre.stallforth@leibniz-hki.de

In Brief

Nonribosomal peptides are a diverse class of ecologically and clinically relevant natural products. Here, Klapper et al. study one of the simplest bacterial nonribosomal peptide synthetases of different *Pseudomonas* strains. A single gene, encoding the monomodular pyreudione synthetase, leads to the production of a variety of bioactive alkaloids.

Highlights

- The pyreudione synthetase is a monomodular NRPS that displays striking plasticity
- Heterologous expression of the pyreudione synthetase was achieved in various hosts
- A functional pyreudione synthetase homolog was found in *Pseudomonas entomophila*
- We performed a phylogenetic analysis of different NRPS thioesterase domains

Klapper et al., 2018, Cell Chemical Biology *25*, 1–7
June 21, 2018
https://doi.org/10.1016/j.chembiol.2018.02.013

CellPress

Please cite this article in press as: Klapper et al., Bacterial Alkaloid Biosynthesis: Structural Diversity via a Minimalistic Nonribosomal Peptide Synthetase, Cell Chemical Biology (2018), https://doi.org/10.1016/j.chembiol.2018.02.013

Cell Chemical Biology

Brief Communication

CellPress

Bacterial Alkaloid Biosynthesis: Structural Diversity via a Minimalistic Nonribosomal Peptide Synthetase

Martin Klapper,[1] Daniel Braga,[2] Gerald Lackner,[2] Rosa Herbst,[1] and Pierre Stallforth[1,3,*]

[1]Junior Research Group Chemistry of Microbial Communication, Leibniz Institute for Natural Product Research and Infection Biology, HKI, Beutenbergstrasse 11a, 07745 Jena, Germany

[2]Junior Research Group Synthetic Microbiology, Leibniz Institute for Natural Product Research and Infection Biology, HKI, Beutenbergstrasse 11a, 07745 Jena, Germany

[3]Lead Contact

*Correspondence: pierre.stallforth@leibniz-hki.de

https://doi.org/10.1016/j.chembiol.2018.02.013

SUMMARY

Chemical and biochemical analyses of one of the most basic nonribosomal peptide synthetases (NRPS) from a *Pseudomonas fluorescens* strain revealed its striking plasticity. Determination of the potential substrate scope enabled us to anticipate novel secondary metabolites that could subsequently be isolated and tested for their bioactivities. Detailed analyses of the monomodular pyreudione synthetase showed that the biosynthesis of the bacterial pyreudione alkaloids does not require additional biosynthetic enzymes. Heterologous expression of a similar and functional, yet cryptic, NRPS of *Pseudomonas entomophila* was successful and allowed us to perform a phylogenetic analysis of their thioesterase domains.

INTRODUCTION

Many therapeutically used drugs contain nonribosomal peptides (NRPs) or derivatives thereof as active ingredients (Sieber and Marahiel, 2005; Süssmuth and Mainz, 2017; Walsh and Fischbach, 2010). Daptomycin, for instance, is an antibacterial nonribosomal cyclic lipopeptide in clinical use against methicillin-resistant *Staphylococcus aureus* (Baltz, 2014; Baltz et al., 2005). Ciclosporin, on the other hand, is a calcineurin inhibitor, indispensable in the prevention of organ rejection in transplant patients (Liu et al., 1991). These peptides are biosynthesized by modular enzyme complexes, so-called nonribosomal peptide synthetases (NRPSs), which link amino acids in an assembly line fashion. Each module can be subdivided into individual domains that catalyze specific steps of the elongation process. Three domains are particularly crucial: the adenylation (A), the thiolation (T), and the condensation (C) domain.

The A domain recruits a specific amino acid monomer and activates it as an aminoacyl adenylate. The sequential order of A domains along the assembly line thus determines, in the majority of cases, the primary sequence of the final peptide. Upon activation, the amino acid is loaded onto a T domain. The C domain then catalyzes the amide bond formation between two amino acids or, in the case of a $C_{starter}$ domain (Rausch et al., 2007), also between a fatty acid and an amino acid. Plasticity of an NRPS can thus arise from the substrate promiscuity or substrate multispecificity of the A and C domains. Eventually the peptide is released, typically via a C-terminal reductase or a thioesterase (TE) domain (Du and Lou, 2010). Different modes of product release have been described, including macrolactonization, macrolactamization, hydrolysis, and Dieckmann cyclization (DC).

Giant multimodular NRPSs have been shown to incorporate, for instance, up to 15 amino acids in the case of kolossin A (Bode et al., 2015). Accordingly, the respective 1.8 MDa enzyme harbors 15 individual modules, which are required to generate this large peptide. While many reports of huge bacterial multimodular NRPSs exist (Hur et al., 2012; Marahiel, 2016), very little is known about the most basic system: the stand-alone monomodular NRPS (Süssmuth and Mainz, 2017). This simple system can incorporate and thus modify in principle a single amino acid. Recently, we showed that one such monomodular NRPS, the pyreudione synthetase Pys from *Pseudomonas fluorescens* HKI0770, enables the formation of the pyreudiones (e.g., pyreudione A, **1**, Figure 1A), a class of potent, bacterially produced amoebicidal alkaloids (Klapper et al., 2016); however, details of their biosynthesis have remained elusive.

RESULTS AND DISCUSSION

The NRPS Pys Is Sufficient for Pyreudione Biosynthesis

Compared with the 1.8 MDa mega enzyme that assembles kolossin A, the minuscule 142 kDa pyreudione synthetase is basically a combination of a starter and a termination module with a C-A-T-TE architecture (Figure 1A). Bioinformatics analysis of the C domain using NaPDoS (Ziemert et al., 2012) clearly confirmed that it belongs to the $C_{starter}$ family, typically involved in linkage of an ACP-bound fatty acid to the downstream amino acid (Rausch et al., 2007). This finding is in line with our proposed biosynthetic model (Klapper et al., 2016).

To test if the *pys* gene is sufficient for the assembly of pyreudiones from simple precursors, we performed the heterologous expression of *pys* in closely related *Pseudomonas protegens* Pf-5, as well as in phylogenetically unrelated *Escherichia coli*

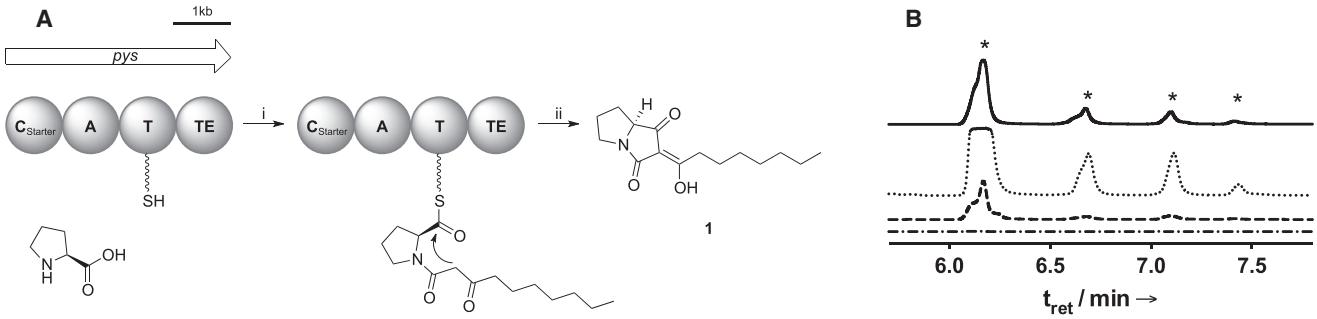

Figure 1. The Monomodular Nonribosomal Peptide Synthetase Pys Catalyzes Pyreudione Formation

(A) Pyreudione A (**1**) biosynthesis: (i) adenylation of L-proline and loading on the T domain, amide bond formation between secondary amine and activated fatty acid; (ii) offloading via DC. (B) HPLC profiles of the native pyreudione producer *P. fluorescens* HKI0770 (top, solid line), and of culture extracts of *E. coli* HM0079 *sfp* pMQ72*pys* (i.e., heterologously expressed *pys,* dotted line) and *P. protegens* Pf-5 pMQ72*pys* (dashed line), control: *P. protegens* Pf-5 wild-type (bottom, dot-dashed line), at λ = 280 nm. * Indicates pyreudiones.

HM0079 *sfp*, which harbors a chromosomally integrated phosphopantethein transferase necessary for NRPS activation (Gruenewald et al., 2004). To this end, we ligated the biosynthetic gene with an engineered ribosomal binding site into the arabinose-inducible vector pMQ72 (Shanks et al., 2006). Upon transformation with the resulting plasmid, we cultured the respective strain in the presence of arabinose. Indeed, the high-performance liquid chromatography (HPLC) profiles of *P. protegens* Pf-5 pMQ72*pys* extract and *E. coli* HM0079 *sfp* pMQ72*pys* extract resembled that of *P. fluorescens* HKI0770 (Figure 1B), with *E. coli* producing even higher amounts of pyreudiones than the native producer. Importantly, pyreudione production in *E. coli* indicates that no other biosynthetic genes but *pys* were required for the biosynthesis of the pyreudiones. Activated acyl precursors thus stem from fatty acid primary metabolism, since the *E. coli* strain used for expression lacks biosynthetic genes that could be present in *Pseudomonas* sp. and provide acyl precursors.

Substrate Multispecificity of the Pys A Domain Enables Access to Novel Pyreudiones

The simplicity of this monomodular NRPS, which effectively activates a single amino acid, is appealing for investigating fundamental mechanistic questions, such as the plasticity of an isolated NRPS module. While substrate promiscuity with respect to the C domain was already reported (Klapper et al., 2016), the A domain could in principle also contribute to product diversification, as shown for instance in the cyclohexadepsipeptide destruxins (Wang et al., 2012) or in the rapamycin biosynthesis (Khaw et al., 1998). We thus analyzed the substrate specificity of the A domain. NRPS substrates can often be predicted by aligning ten conserved residues (A domain signature) in the substrate-binding pockets of A domains (Stachelhaus et al., 1999). Based on our previous biosynthetic model (Klapper et al., 2016), the Pys A domain selects and activates proline. However, the A domain signature of Pys (D-M-L-V-M-G-V-F-A-K) bears no resemblance to the consensus A domain signature for proline described by Stachelhaus et al. (1999) (D-V-Q-L-I-A-H-V-V-K). Other NRPS analysis programs also failed to predict the A domain specificity (Bachmann and Ravel, 2009; Röttig et al., 2011). This led us to biochemically determine the substrate scope of the Pys A domain using an ATP/[^{32}P]pyrophosphate exchange assay. Thus, a C-A didomain protein bearing an N-terminal His-tag was recombinantly produced. All canonical amino acids and L-ornithine were subdivided into five pools. Every pool was then individually subjected to the exchange assay in the presence of the C-A didomain. Incorporation of [^{32}P] into ATP was observed when pool II was added to the exchange assay (Figure 2A). The A domain was selective for L-proline, when tested individually. No other constituent of pool II led to the incorporation of [^{32}P] into ATP, nor did D-proline serve as substrate for the A domain. We then proceeded to investigate if the A domain would accept amino acids bearing some structural similarity to proline, such as pipecolic acid (**2**), azetidine 2-carboxylic acid (**3**), pyrrole-3-carboxylic acid (**4**), pyrrole-2-carboxylic acid (**5**), L-hydroxyproline (**6**), and L-oxoproline (**7**). Interestingly, most of these substrates were accepted by the Pys A domain (Figure 2B).

Since many microorganisms have the capacity to generate L-pipecolic acid (Chang and Adams, 1971), we wondered if the corresponding pyreudione congener, indolizidine dione **8** (Figure 2C), could be endogenously produced by *P. fluorescens* HKI0770. Importantly, genome mining of *P. fluorescens* HKI0770 allowed the identification of Δ1-piperideine-2-carboxylate (P2C) reductase, which catalyzes the reduction of P2C into pipecolic acid via the P2C route (Chang and Adams, 1971). Liquid chromatography-mass spectrometry-based identification of a compound with *m/z* 280.2 $[M + H]^+$ gave a first indication that the anticipated novel alkaloid may be present, albeit in low abundance. Chemical synthesis of the corresponding standard using a previously established synthetic approach (Klapper et al., 2016), starting from L-pipecolic acid (Figure 2D), confirmed endogenous production of pyreudione E (**8**), the indolizidine analog of pyreudione A (**1**), by the native producer.

Due to their low production rates, isolation of indolicidine congeners was impossible under standard conditions. Increasing the concentration of L-pipecolic acid in the culture medium by exogenous supplementation, however, led to an increase in the production of pyreudione E (**8**) and other indolizidine diones. Eventually, we were able to isolate pyreudiones E to H (**8**–**11**) from *P. fluorescens* HKI0770 in sufficient quantities for

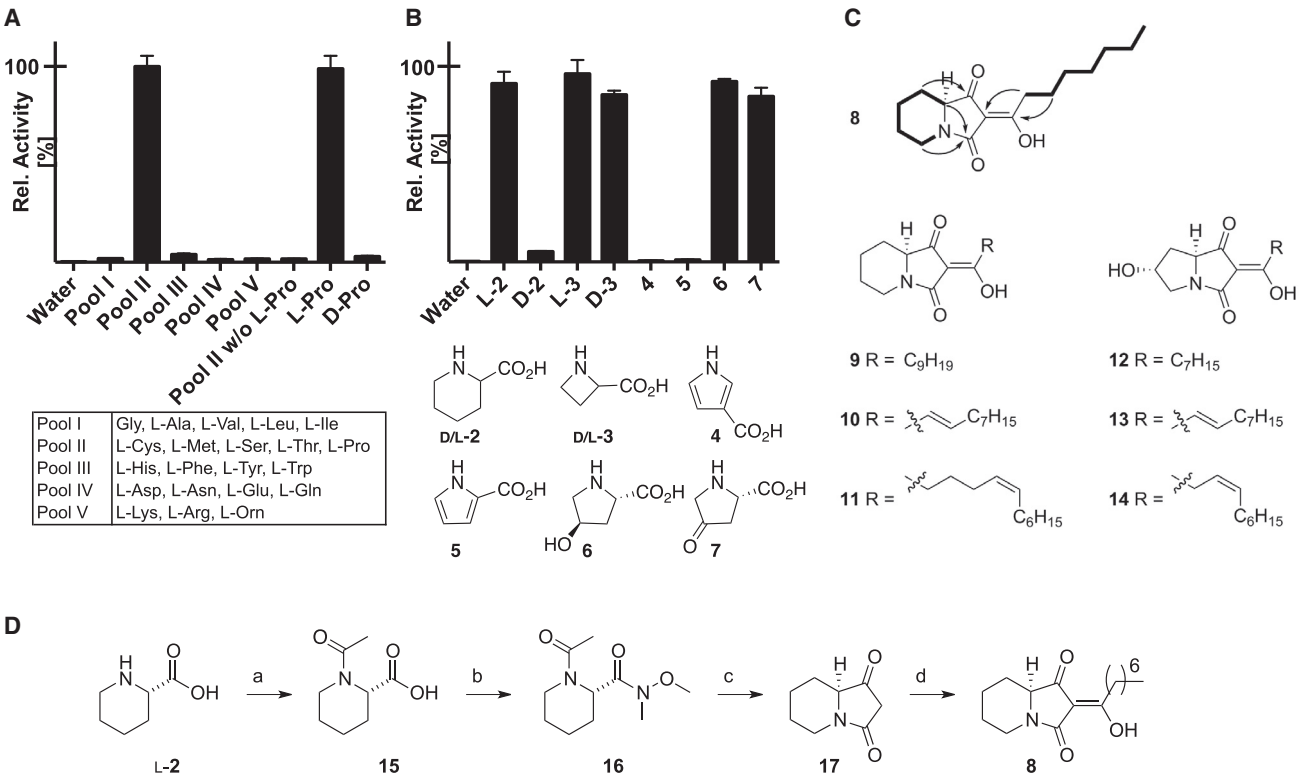

Figure 2. Substrate Multispecificity of the Pys A Domain Enables Access to Novel Pyreudiones

(A and B) Substrate specificities of the Pys A domain determined by the ATP/[^{32}P]pyrophosphate exchange assay. The substrate with highest activity was set to 100%. The average of three replicates is shown. Error bars represent SD. (A) The canonical amino acids (including L-ornithine) were divided into five pools that were individually tested. Of these substrates, only L-proline was accepted as substrate. (B) Substrates bearing structural similarity with L-proline were accepted by the A domain.

(C) Chemical structures of novel pyreudiones derived from L-pipecolic acid (**8**–**11**) and L-hydroxyproline (**12**–**14**).

(D) Synthesis of pyreudione E (**8**). Reagents and conditions: a. Ac_2O, THF, $NaHCO_3$, RT; b. NEt_3, EDCI, *N*,*O*-dimethyl hydroxylamine, CH_2Cl_2, 0°C; c. LHMDS, THF, −78°C; d. EDCI, CH_2Cl_2, $CH_3(CH_2)_6CO_2H$, DMAP, RT. Overall yield over four steps from L-pipecolic acid 11%. See Supplemental Information for detailed procedures.

their structure elucidation. Nuclear magnetic resonance (NMR) spectroscopic data for the main metabolite matched those of synthesized **8**, while the structures of the other congeners were determined using one- and two-dimensional NMR spectroscopy and high-resolution mass spectrometry (HRMS). Interestingly, we could not identify any azetidine-based pyreudiones by supplementing azetidine-2-carboxylic acid to the culture medium. Feeding either L-hydroxy-or L-oxoproline, however, led in both cases to the production of pyreudiones I to K (**12**–**14**), which were otherwise not produced by *P. fluorescens* HKI0770 (Figure 2C).

Antimicrobial Activity

The main congeners pyreudione E (**8**) and pyreudione I (**12**) were tested for amoebicidal activity, as well as for antimicrobial activity. Interestingly, only naturally occurring pyreudione E (**8**) displayed amoebicidal activity comparable to previously reported pyreudiones (1–11 μg/mL or 3–41 μM, respectively, Klapper et al., 2016) with half maximal inhibitory concentration (IC_{50}) (*Dictyostelium discoideum*) = 6 μg/mL (21 μM). Further antimicrobial testing revealed an antibiotic activity of pyreudione E (**8**) against *Mycobacterium aurum* and *Mycobacterium vaccae* with minimum inhibitory concentration (MIC) = 12.5 μg/mL (45 μM), whereas pyreudione I (**12**) did not show any antimicrobial activity (MIC >100 μg/mL). Short-chain analogs of pyreudione A (**1**) with six or fewer carbon atoms in the alkyl side chain also did not show any antimicrobial activity (Klapper et al., 2016). Notably, pyreudione A derivative containing a C12 alkyl chain displayed strongly increased activity against *M. vaccae* and *M. aurum* with MIC = 0.4 μg/mL (1.2 μM). The influence of the compound's lipophilicity on bioactivity due to variations in alkyl chain lengths or the presence of an additional hydroxyl group (pyreudione I, **12**), needs to be addressed in future structure-activity relationship and mode-of-action studies.

Expression Analysis of *pys*-Homolog pys_{PENT} from *Pseudomonas entomophila*

The prerequisite for the production of a diversity of pyreudiones is not only a multispecific A domain, but the TE domain has to promote the DC irrespective of the amino acid loaded on the T domain. In order to decipher the evolutionary history of the Pys TE domain, we investigated the presence of C-A-T-TE-type monomodular NRPS in other bacterial species using a

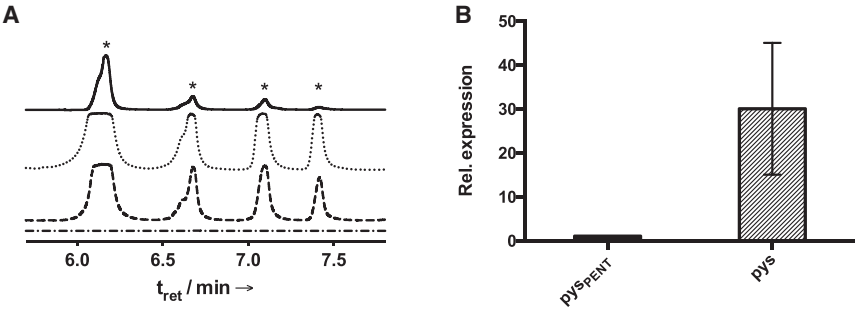

Figure 3. Expression Analysis of a *pys*-Homolog from *P. entomophila* (pys_{PENT})

(A) HPLC profiles of the native pyreudione producer *P. fluorescens* HKI0770 (top, solid line), and of culture extracts of *E. coli* HM0079 *sfp* pMQ72pys_{PENT} (dotted line) and *P. protegens* Pf-5 pMQ72pys_{PENT} (dashed line), control: *P. entomophila* wild-type (bottom, dot-dashed line) at λ = 280 nm, * indicates pyreudiones.

(B) RT-qPCR expression analysis of pys_{PENT} of *P. entomophila* (DSMZ 28517) and *pys* of *P. fluorescens* HKI0770, respectively. Both strains were cultured in SM/5 medium to OD600 = 1. Expression level of pys_{PENT} was set to 1. The respective *rpoD* gene was used for internal normalization. The average of three independent biological replicates is shown. Three technical replicates were conducted for each biological replicate. Error bars represent SD of biological replicates.

protein-protein BLAST search of Pys against the non-redundant database of NCBI. We found a variety of bacteria that harbor similar C-A-T-TE-type NRPSs (Table S2); however, none of the genes had been linked to a secondary metabolite so far.

The monomodular NRPS of the insect pathogen *Pseudomonas entomophila* L48 (Pys_{PENT}) showed 81% similarity to that of *P. fluorescens* HKI0770. Moreover, the A domain signatures of both NRPSs were identical, suggesting a similar substrate scope of Pys and Pys_{PENT}. Due to this high similarity, sequenced *P. entomophila* (DSMZ 28517) appeared to be a good candidate to search for the production of pyreudiones or analogs thereof. We cultured *P. entomophila* in various media and extracted the cultures with ethyl acetate. Unfortunately, we could not detect the presence of any compounds with a similar UV absorbance spectrum to the pyreudiones in these culture extracts (Figure 3A). Transcriptional analysis of pys_{PENT} in comparison to *pys* by quantitative reverse transcription PCR (RT-qPCR) showed that the former was 30-fold less expressed in SM/5 medium (Figure 3B), a medium that led to particularly good production rates of pyreudiones in *P. fluorescens* HKI0770.

Finally, we aimed at expressing pys_{PENT} in *P. protegens* Pf-5 and *E. coli* HM0079 *sfp* (using pMQ72pys_{PENT}). Eventually, this approach led to the production of pyreudiones A–D (Klapper et al., 2016) as produced by *P. fluorescens* HKI0770 (Figure 3A). Thus, despite being fully functional, pys_{PENT} is silent in *P. entomophila.* Since transformation of *P. entomophila* with pMQ72pys_{PENT} led to the production of the same set of pyreudiones, it is likely that *P. entomophila* requires specific environmental cues in order to activate pys_{PENT} expression. The established expression system is thus suitable for expressing other homologous monomodular NRPS with so far unknown products in future studies.

Phylogenetic Analyses of TE-like Domains of Bacterial NRPS

With the amino acid sequences of Pys and Pys_{PENT}, as well as 24 TE domain sequences of other representative NRPSs, we constructed a maximum likelihood tree (Figure 4). As expected, both TE domains of Pys and Pys_{PENT} were phylogenetically closely related. In NRPS, TE domains typically catalyze the "canonical" release of the NRP via hydrolysis or macrocyclization, as seen for cyclic lipopeptides (Du and Lou, 2010). For the described monomodular NRPSs, however, a DC yields an *E/Z* mixture of the tetramic acids (with the *Z* isomer being the major form). While it remains unclear whether the TE domain catalyzes the cyclization during the pyreudione biosynthesis, TE-like domains with DC activity have been described. TE-like domains related to the heat-stable antifungal factor synthetase from *Lysobacter enzymogenes* (Du and Lou, 2010; Yu et al., 2006) and free-standing TE-like domains similar to LipX2 of the lipomycin pathway of *Streptomyces aureofaciens* for instance were reported. However, neither of the two pyreudione synthetase TE domains shows a close phylogenetic relationship to the above-mentioned groups. Despite intensive efforts, we could not detect any specific motif shared by all TE domains that yield DC products. Interestingly, the pyreudione synthetase TE domains are more closely related to the TE of serrawettin synthetase SwrW, which exhibits the identical C-A-T-TE domain architecture. Yet, this TE supports macrocyclization, rather than DC. Still, it is unusual in that it catalyzes a dimerization, most likely via two following transesterification steps (Li et al., 2005). Notably, tetramic acid formation by a TE domain can alternatively proceed via lactamization as proposed for the hybrubins (HbnA) (Zhao et al., 2016).

SIGNIFICANCE

Nonribosomal peptides (NRPs) are important antibiotics, anticancer agents, or immunomodulators. A detailed biosynthetic analysis of a strongly bioactive class of NRPs enabled the identification and isolation of novel alkaloids that would otherwise have been overlooked. The amoebicidal pyreudione alkaloids are formed by the sole action of the monomodular nonribosomal peptide synthetase (NRPS) Pys. A homologous NRPS in *P. entomophila* (Pys_{PENT}), which has 81% similarity to Pys, appears silent under different culture conditions. Heterologous expression of *pys* and pys_{PENT} in *E. coli* and different *Pseudomonas* species, however, led to the production of the same set of pyreudiones as seen in *P. fluorescens* HKI0770. The simplicity and plasticity of this stand-alone monomodular NRPS is a great system for subsequent bioengineering of NRPSs in order to access a variety of new natural products. Using the established expression system, the substrate scopes of other monomodular NRPSs,

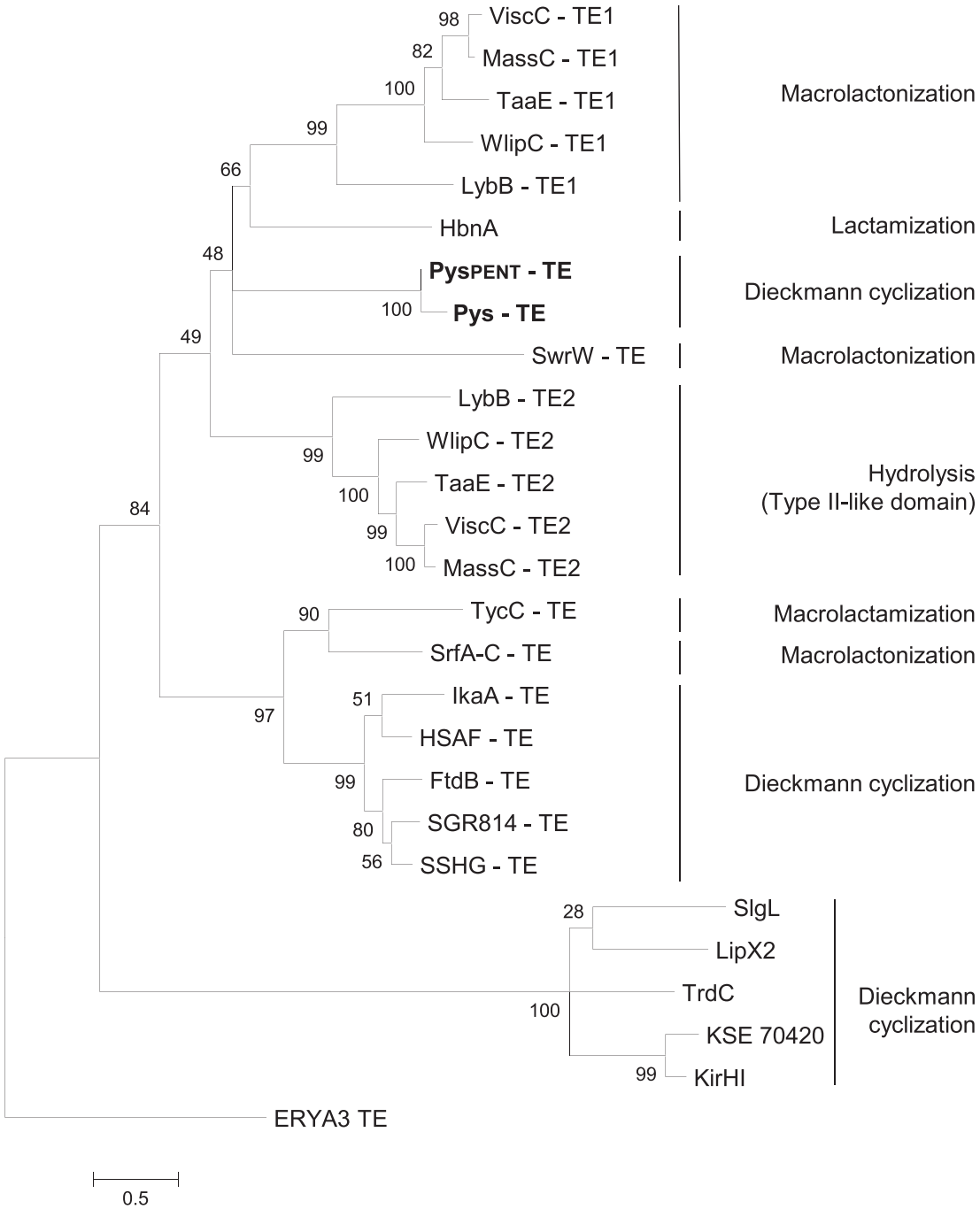

Figure 4. Phylogenetic Analysis of 26 TE-like Domains of Bacterial NRPS

The observed mode of release, such as macrolactonization, DC, or hydrolysis, is indicated. The scale bar represents 50 substitutions per 100 amino acids. Bootstrap values higher than 45% are shown. The respective proteins and the resulting nonribosomal peptides are shown in Table S3.

considering both the C domain and A domain specificity, can now be investigated. Importantly, this class of enzymes seems to be widely spread across the bacterial kingdom and their biosynthetic products await discovery. Identification of the presumed environmental cues for their activation would enhance our knowledge of their ecological functions.

STAR★METHODS

Detailed methods are provided in the online version of this paper and include the following:

- KEY RESOURCES TABLE
- CONTACT FOR REAGENT AND RESOURCE SHARING

SUPPLEMENTAL INFORMATION

Supplemental Information includes two figures, four tables, and one data file and can be found with this article online at https://doi.org/10.1016/j.chembiol.2018.02.013.

ACKNOWLEDGMENTS

We thank A. Perner, H. Heinecke, and Dr. S. Schieferdecker (Hans Knöll Institute, Jena) for MS and NMR measurements; Dr. M. Roth, K. Willing, M. Steinacker, J. Schönemann, and P. Berthel for large-scale fermentations; C. Weigel for antimicrobial activity testing; and H. Kries for providing *E. coli* HM0079 *sfp*. This work was funded by the DFG (STA 1431/2-1, and CRC 1127 ChemBioSys) We are also grateful for financial support from the Leibniz Association, Carl Zeiss Foundation (D.B., G.L.), an Aventis Foundation PhD fellowship (M.K.), and for a fellowship of the Daimler and Benz Foundation (P.S.).

AUTHOR CONTRIBUTIONS

P.S., M.K., D.B., R.H., and G.L. planned experiments; M.K., D.B., and G.L. performed experiments (protein isolation, ATP-PP_i exchange assay and phylogeny: D.B., G.L.); P.S. and M.K. wrote the manuscript; D.B., G.L., and R.H. edited the manuscript.

DECLARATION OF INTERESTS

The authors declare no competing interests.

Received: December 13, 2017
Revised: January 26, 2018
Accepted: February 22, 2018
Published: March 29, 2018

REFERENCES

Bachmann, B.O., and Ravel, J. (2009). Methods for in silico prediction of microbial polyketide and nonribosomal peptide biosynthetic pathways from DNA sequence data. Methods Enzymol. *458*, 181–217.

Baltz, R.H. (2014). Combinatorial biosynthesis of cyclic lipopeptide antibiotics: a model for synthetic biology to accelerate the evolution of secondary metabolite biosynthetic pathways. ACS Synth. Biol. *3*, 748–758.

Baltz, R.H., Miao, V., and Wrigley, S.K. (2005). Natural products to drugs: daptomycin and related lipopeptide antibiotics. Nat. Prod. Rep. *22*, 717–741.

Bode, H.B., Brachmann, A.O., Jadhav, K.B., Seyfarth, L., Dauth, C., Fuchs, S.W., Kaiser, M., Waterfield, N.R., Sack, H., Heinemann, S.H., and Arndt, H.D. (2015). Structure elucidation and activity of kolossin A, the d-/l- pentadecapeptide product of a giant nonribosomal peptide synthetase. Angew. Chem. Int. Ed. *54*, 10352–10356.

Bradford, M.M. (1976). A rapid and sensitive method for the quantitation of microgram quantities of protein utilizing the principle of protein-dye binding. Anal. Biochem. *72*, 248–254.

Chang, Y.F., and Adams, E. (1971). Induction of separate catabolic pathways for L- and D-lysine in *Pseudomonas putida*. Biochem. Biophys. Res. Commun. *45*, 570–577.

Clinical and Laboratory Standards Institute. (2006). Methods for Dilution Antimicrobial Susceptibility Tests for Bacteria that Grow Aerobically, Approved Standard, *Vol. 26*, Fourth Edition (Clinical and Laboratory Standards Institute).

Du, L., and Lou, L. (2010). PKS and NRPS release mechanisms. Nat. Prod. Rep. *27*, 255–278.

Edgar, R.C. (2004). MUSCLE: multiple sequence alignment with high accuracy and high throughput. Nucleic Acids Res. *32*, 1792–1797.

Gervais, A.L., Marques, M., and Gaudreau, L. (2010). PCRTiler: automated design of tiled and specific PCR primer pairs. Nucleic Acids Res. *38*, W308–W312.

Gomi, S., Imamura, K., Yaguchi, T., Kodama, Y., Minowa, N., and Koyama, M. (1994). PF1018, a novel insecticidal compound produced by *Humicola* sp. J. Antibiot. (Tokyo) *47*, 571–580.

Gruenewald, S., Mootz, H.D., Stehmeier, P., and Stachelhaus, T. (2004). In vivo production of artificial nonribosomal peptide products in the heterologous host *Escherichia coli*. Appl. Environ. Microbiol. *70*, 3282–3291.

Hur, G.H., Vickery, C.R., and Burkart, M.D. (2012). Explorations of catalytic domains in non-ribosomal peptide synthetase enzymology. Nat. Prod. Rep. *29*, 1074–1098.

Huson, D.H. (1998). SplitsTree: analyzing and visualizing evolutionary data. Bioinformatics *14*, 68–73.

Jeong, Y.C., Bikadi, Z., Hazai, E., and Moloney, M.G. (2014). A detailed study of antibacterial 3-acyltetramic acids and 3-acylpiperidine-2,4-diones. ChemMedChem *9*, 1826–1837.

Khaw, L.E., Böhm, G.A., Metcalfe, S., Staunton, J., and Leadlay, P.F. (1998). Mutational biosynthesis of novel rapamycins by a strain of *Streptomyces hygroscopicus* NRRL 5491 disrupted in *rapL*, encoding a putative lysine cyclodeaminase. J. Bacteriol. *180*, 809–814.

Klapper, M., Götze, S., Barnett, R., Willing, K., and Stallforth, P. (2016). Bacterial alkaloids prevent amoebal predation. Angew. Chem. Int. Ed. *55*, 8944–8947.

Le, S.Q., and Gascuel, O. (2008). An improved general amino acid replacement matrix. Mol. Biol. Evol. *25*, 1307–1320.

Li, H., Tanikawa, T., Sato, Y., Nakagawa, Y., and Matsuyama, T. (2005). *Serratia marcescens* gene required for surfactant serrawettin W1 production encodes putative aminolipid synthetase belonging to nonribosomal peptide synthetase family. Microbiol. Immunol. *49*, 303–310.

Liu, J., Farmer, J.D., Lane, W.S., Friedman, J., Weissman, I., and Schreiber, S.L. (1991). Calcineurin is a common target of cyclophilin-cyclosporin A and FKBP-FK506 complexes. Cell *66*, 807–815.

Livak, K.J., and Schmittgen, T.D. (2001). Analysis of relative gene expression data using real-time quantitative PCR and the $2^{-\Delta\Delta C}{}_T$ method. Methods *25*, 402–408.

Marahiel, M.A. (2016). A structural model for multimodular NRPS assembly lines. Nat. Prod. Rep. *33*, 136–140.

Murray, A., Proctor, G.R., and Murray, P.J. (1996). An efficient route to the pyrrolizidine ring system via an N-acyl anion cyclisation process. Tetrahedron *52*, 3757–3766.

Pizzorno, M.T., and Albonico, S.M. (1977). Novel synthesis of 5,6,7,8-tetrahydroindolizine. J. Org. Chem. *42*, 909–910.

Rausch, C., Hoof, I., Weber, T., Wohlleben, W., and Huson, D.H. (2007). Phylogenetic analysis of condensation domains in NRPS sheds light on their functional evolution. BMC Evol. Biol. *7*, 78.

Röttig, M., Medema, M.H., Blin, K., Weber, T., Rausch, C., and Kohlbacher, O. (2011). NRPSpredictor2—a web server for predicting NRPS adenylation domain specificity. Nucleic Acids Res. *39*, W362–W367.

Shanks, R.M., Caiazza, N.C., Hinsa, S.M., Toutain, C.M., and O'Toole, G.A. (2006). *Saccharomyces cerevisiae*-based molecular tool kit for manipulation of genes from gram-negative bacteria. Appl. Environ. Microbiol. *72*, 5027–5036.

Sieber, S.A., and Marahiel, M.A. (2005). Molecular mechanisms underlying nonribosomal peptide synthesis: approaches to new antibiotics. Chem. Rev. *105*, 715–738.

Stachelhaus, T., Mootz, H.D., and Marahiel, M.A. (1999). The specificity-conferring code of adenylation domains in nonribosomal peptide synthetases. Chem. Biol. *6*, 493–505.

Süssmuth, R.D., and Mainz, A. (2017). Nonribosomal peptide synthesis-principles and prospects. Angew. Chem. Int. Ed. *56*, 3770–3821.

Tamura, K., Stecher, G., Peterson, D., Filipski, A., and Kumar, S. (2013). MEGA6: molecular evolutionary genetics analysis version 6.0. Mol. Biol. Evol. *30*, 2725–2729.

Walsh, C.T., and Fischbach, M.A. (2010). Natural products version 2.0: connecting genes to molecules. J. Am. Chem. Soc. *132*, 2469–2493.

Wang, B., Kang, Q., Lu, Y., Bai, L., and Wang, C. (2012). Unveiling the biosynthetic puzzle of destruxins in *Metarhizium* species. Proc. Natl. Acad. Sci. USA *109*, 1287–1292.

Wiegand, I., Hilpert, K., and Hancock, R.E. (2008). Agar and broth dilution methods to determine the minimal inhibitory concentration (MIC) of antimicrobial substances. Nat. Protoc. *3*, 163–175.

Yu, F., Zaleta-Rivera, K., Zhua, X., Huffman, J., Millet, J.C., Harris, S.D., Yuen, G., Li, X.C., and Du, L. (2006). Structure and biosynthesis of heat-stable antifungal factor (HSAF), a broad-spectrum antimycotic with a novel mode of action. Antimicrob. Agents Chemother. *51*, 64–72.

Zhao, Z., Shi, T., Xu, M., Brock, N.L., Zhao, Y.-L., Wang, Y., Deng, Z., Pang, X., and Tao, M. (2016). Hybrubins: bipyrrole tetramic acids obtained by crosstalk between a truncated undecylprodigiosin pathway and heterologous tetramic acid biosynthetic genes. Org. Lett. *18*, 572–575.

Ziemert, N., Podell, S., Penn, K., Badger, J.H., Allen, E., and Jensen, P.R. (2012). The natural product domain seeker NaPDoS: a phylogeny based bioinformatic tool to classify secondary metabolite gene diversity. PLoS One *7*, e34064.

STAR★METHODS

KEY RESOURCES TABLE

REAGENT or RESOURCE	SOURCE	IDENTIFIER
Bacterial and Virus Strains		
Pseudomonas fluorescens HKI0770 Δ*clp*	Klapper et al., 2016	N/A
Escherichia coli Top10	ThermoFisher	Cat#C404010
Escherichia coli ET12567 pUZ8002	Kothe Lab	N/A
Pseudomonas protegens Pf-5	Clardy Lab	N/A
Pseudomonas entomophila DSM28517	DSMZ	DSM28517
Escherichia coli HM0079 *sfp*	Kries Lab, Gruenewald et al., 2004	N/A
Escherichia coli KRX	Promega	Cat#L3002
Bacillus subtilis 6633	HKI microbial strain collection	N/A
Staphylococcus aureus SG511	HKI microbial strain collection	N/A
Staphylococcus aureus SG511	HKI microbial strain collection	N/A
Escherichia coli SG458	HKI microbial strain collection	N/A
Pseudomonas aeruginosa K799/61	HKI microbial strain collection	N/A
Mycobacterium vaccae 10670	HKI microbial strain collection	N/A
Mycobacterium aurum SB66	HKI microbial strain collection	N/A
Sporobolomyces salmonicolor 549	HKI microbial strain collection	N/A
Candida albicans C.A.	HKI microbial strain collection	N/A
Penicillum notatum JP36	HKI microbial strain collection	N/A
Biological Samples		
gDNA of *Pseudomonas fluorescens* HKI0770	Klapper et al., 2016	N/A
gDNA of *Pseudomonas entomophila* DSM28517	This study	N/A
Chemicals, Peptides, and Recombinant Proteins		
CutSmart® Buffer	New England Biolabs	Cat#B7204S
XmaI	New England Biolabs	Cat#R0180S
SalI-HF®	New England Biolabs	Cat#R3138S
HindIII-HF®	New England Biolabs	Cat#R3104S
L-rhamnose	VWR	Cat#ICNA0210280980;CAS:10030-85-0
L-arabinose	VWR	Cat#1B1473;CAS:5328-37-0
Imidazole	TCI	Cat#I0001;CAS:288-32-4
Chloroform, deuterated	VWR Chemicals	Cat#87153.0006;CAS:865-49-6
Gentamicinsulfate solution (gentamicin)	Carl Roth	Cat#2475.1;CAS:1405-41-0
Kanamycinsulfate (kanamycin)	Carl Roth	Cat#T832.1;CAS:25389-94-0
Chloramphenicol	Carl Roth	Cat#3886.2;CAS:56-75-7
Ampicillin sodium salt (ampicillin)	Carl Roth	Cat#K029.1
SM/5	Formedium™	Cat#SMB50102
Protino nickel-nitrilo acetic resin	Macherey-Nagel	Cat#745400.500
PD-10 desalting column	GE Healthcare	Cat#17-0851-01
Pys N-His_6 C-A didomain	This study	N/A
[^{32}P]pyrophosphate	Perkin Elmer	Cat#NEX019001MC
Scintillation liquid	Carl Roth	Cat#0016.3
L-proline	TCI	Cat#P0481;CAS:147-85-3
D-proline	Alfa Aesar	Cat#A10682;CAS:344-25-2
L-pipecolic acid **2**	Carbolution Chemicals	Cat#CC10002;CAS:3105-95-1
D-pipecolic acid **2**	Carbolution Chemicals	Cat#CC10003;CAS:1723-00-8
L-azetidine 2-carboxylic acid **3**	Fluorochem Ltd	Cat#093784;CAS:2133-34-8

(*Continued on next page*)

Continued

REAGENT or RESOURCE	SOURCE	IDENTIFIER
D-azetidine 2-carboxylic acid **3**	Fluorochem Ltd	Cat#040006;CAS:7729-30-8
Pyrrole-2-carboxylic acid **5**	Sigma Aldrich	CAT#P73609;CAS:634-97-9
Pyrrole-3-carboxylic acid **4**	Sigma Aldrich	CAT#689416;CAS:931-03-3
L-hydroxyproline **6**	Sigma Aldrich	CAT#H54409;CAS:51-35-4
L-oxoproline **7**	Alfa Chemistry	Cat#ACM4347186;CAS:4347-18-6
HyperSep™ 1g C18 column	ThermoFisher Scientific	Cat#60108-301
Critical Commercial Assays		
QIAprep® Spin Miniprep Kit	Qiagen	Cat#27106
GeneJET Gel Extraction Kit	Thermo Fisher Scientific	Cat#K0692
QIAamp DNA Mini Kit	Qiagen	Cat#51304
Q5® High-Fidelity 2x Master Mix	New England Biolabs	Cat#M0492S
DreamTaq Green PCR Master Mix 2x	Thermo Scientific	Cat#K1082
Gibson assembly® Master Mix	New England Biolabs	Cat#E2611S
Q5® Site-Directed Mutagenesis Kit	New England Biolabs	Cat#E0544S
RNeasy® Mini Kit	Qiagen	Cat#74104
RNAprotect® Bacteria Reagent	Qiagen	Cat#76506
TURBO DNA-free™ kit	Thermo Fisher Scientific	Cat#AM1907
RevertAid Reverse Transcriptase	Thermo Fisher Scientific	Cat#EP0442
PowerUpTM SYBR® Green Master Mix	Thermo Fisher Scientific	Cat#A25742
DNA Sanger sequencing	LGC Genomics, Berlin	N/A
Deposited Data		
WP_064118616, Pys protein sequence	NCBI	https://www.ncbi.nlm.nih.gov/protein/ WP_064118616
WP_011533552, Pys_{PENT} protein sequence	NCBI	https://www.ncbi.nlm.nih.gov/protein/WP_011533552
Experimental Models: Cell Lines		
Dictyostelium discoideum AX2	dictybase.org	N/A
Experimental Models: Organisms/Strains		
Pseudomonas fluorescens HKI0770	Klapper et al., 2016	N/A
Escherichia coli Top10 pMQ72*pys*	This study	N/A
Escherichia coli Top10 pMQ72pys_{PENT}	This study	N/A
Escherichia coli ET12567 pUZ8002 pMQ72pys_{PENT}	This study	N/A
Escherichia coli ET12567 pUZ8002 pMQ72pys_{PENT}	This study	N/A
Pseudomonas protegens Pf-5 pMQ72*pys*	This study	N/A
Pseudomonas protegens Pf-5 pMQ72pys_{PENT}	This study	N/A
Pseudomonas entomophila pMQ72pys_{PENT}	This study	N/A
Escherichia coli HM0079 *sfp* pMQ72*pys*	This study	N/A
Escherichia coli HM0079 *sfp* pMQ72pys_{PENT}	This study	N/A
Escherichia coli KRX pBK01	This study	N/A
Oligonucleotides		
Primers for all cloning procedures: *c.f.* Table S1	Invitrogen ThermoFisher Scientific (Darmstadt)	N/A
Random Hexamers	Thermo Fisher Scientific	Cat#N8080127
Recombinant DNA		
pMQ97_gfp	Shanks et al., 2006	N/A
pMQ72	Shanks et al., 2006	N/A
pMQ72*rbs*	This study	N/A
pMQ72*pys*	This study	N/A
pMQ72pys_{PENT}	This study	N/A

(*Continued on next page*)

Continued

REAGENT or RESOURCE	SOURCE	IDENTIFIER
pET28a(+)	Novagen/Merck	Cat#69864
pBK01	This study	N/A
Software and Algorithms		
Gibson Assembly	New England Biolabs	http://nebuilder.neb.com
NEBaseChanger™	New England Biolabs	https://nebasechanger.neb.com/
NCBI Protein Blast	NCBI	https://blast.ncbi.nlm.nih.gov/Blast.cgi?PAGE=Proteins
PCRTiler	PCRTiler v1.42, Gervais et al., 2010	http://pcrtiler.genap.ca/PCRTiler/
ChemBioDraw Ultra 13.0	PerminElmer	http://www.cambridgesoft.com/
Geneious 11	Biomatters	https://www.geneious.com/
Topspin 3.2	Bruker	https://www.bruker.com/
GraphPad Prism, Version 5.03	Graphpad Software, Inc.	https://www.graphpad.com/

CONTACT FOR REAGENT AND RESOURCE SHARING

Further information and requests for resources and reagents should be directed to and will be fulfilled by the Lead Contact, Dr. Pierre Stallforth (pierre.stallforth@leibniz-hki.de).

EXPERIMENTAL MODEL AND SUBJECT DETAILS

Dictyostelium discoideum AX2

Axenic *Dictyostelium discoideum* AX2 cells (dictybase.org) were cultured in HL/5 liquid medium (Formedium™, UK). An aliquot (5–10 μL) of a *D. discoideum* spore glycerol stock was added to 10 mL HL5 medium in a cell culture plate (Sarstedt, Germany). After five days at 22°C, when confluency was reached, the cells were detached by gentle pipetting and split (1/10) into a new cell culture plate. Adherent cells were detached and used to inoculate a continuous shaking culture (22°C, 135 rpm). Cultures were split after 3 – 4 days to keep the cells in their exponential growth phase. Cultures were renewed monthly from spore stocks.

Pseudomonas Strains

Pseudomonas fluorescens HKI0770, *Pseudomonas fluorescens* HKI0770 Δ*clp*, *Pseudomonas entomophila* DSM28517 and *Pseudomonas protegens* Pf-5 were propagated on SM/5 solid agar or grown in SM/5 liquid medium (Formedium™, UK) on a gyratory shaker at 160 rpm at 22°C unless otherwise noted.

When required, media were supplemented with gentamicin (75 μg/mL for *P. entomophila* DSM28517 mutants, or 50 μg/mL for *P. protegens* Pf-5 mutants, Carl Roth, Germany), kanamycin (50 μg/mL, Carl Roth, Germany), chloramphenicol (50 μg/mL, Carl Roth, Germany), and ampicillin (100 μg/mL, Carl Roth, Germany).

Escherichia coli Strains

Escherichia coli strains were cultured at 37°C in LB liquid or on solid agar medium (Carl Roth, Germany). When required, media were supplemented with gentamicin (15 μg/mL, Carl Roth, Germany), kanamycin (50 μg/mL, Carl Roth, Germany), and chloramphenicol (50 μg/mL, Carl Roth, Germany).

METHOD DETAILS

General Biological Methods

Glycerol stocks of bacterial strains were prepared by mixing 1 mL overnight culture of the respective strain with 0.5 mL of 60% (v/v) *aq.* glycerol and stored at –80°C.

Plasmid constructions were carried out using the Gibson Assembly method (New England Biolabs, software: http://nebuilder.neb.com). Plasmids were isolated using QIAprep® Spin Miniprep Kit (Qiagen), and PCR reaction products were purified for subsequent cloning and sequencing by gel extraction using GeneJET Gel Extraction Kit (Thermo Scientific). PCR reactions were carried out using Q5® High-Fidelity 2x Master Mix (New England Biolabs) for applications requiring high fidelity such as sequencing and cloning, for other applications (*e.g.* colony PCR) DreamTaq Green PCR Master Mix 2x (Thermo Scientific, Darmstadt) was used. Restriction digests were carried out using NEB restriction enzymes and CutSmart® Buffer (New England Biolabs). Genomic DNA was isolated from 3 mL bacterial overnight culture in SM/5 medium using the QIAamp DNA Mini Kit (Qiagen). Oligonucleotides used in this study were purchased from Invitrogen (ThermoFisher Scientific, Darmstadt). DNA Sanger sequencing was performed by LGC Genomics, Berlin.

Instrumentation

All 1D (^{1}H, ^{13}C) and 2D NMR spectra (^{1}H-^{1}H COSY, HSQC, HMBC, NOESY, homonuclear *J*-resolved ^{1}H) were recorded in deuterated chloroform (Carl Roth, Germany) on Bruker AVANCE III 300, 500 and 600 MHz (equipped with a Bruker Cryo Platform) instruments. The chemical shifts are reported in parts per million (δ) relative to the resonance of the residual solvent (δ $CHCl_3$ = 7.26/77.0 for ^{1}H and ^{13}C spectra, respectively). Coupling constants (*J*) are reported in Hertz (Hz). HRESI-MS measurements were conducted on a Thermo Fisher Exactive Orbitrap either by direct injection or in combination with a Thermo Accela HPLC system. The system is equipped with an electrospray ion source and a Betasil 100-3 C18 column (150 × 2.1 mm). The following elution gradient was used: solvent A: H_2O + 0.1% HCOOH, solvent B: acetonitrile, gradient: 5% B for 1 min, 5% to 98% B in 15 min, 98% B for 15 min, flow rate: 0.2 mL/min, injection: 5 μL. UHPLC-MS was performed on a Shimadzu System (LC-30AD, SPD-M30A, LCMS-2020). The system is equipped with an electrospray ion source and a Kinetex® C18 column (50 × 2.1 mm, 1.7 μm, 100 Å, Phenomenex). The following elution gradient was used: solvent A: H_2O + 0.1% HCOOH, solvent B: acetonitrile + 0.1% HCOOH, gradient: 10% B for 0.5 min, 10% to 100% B in 8 min, 100% B for 3 min, flow rate: 0.7 mL/min, injection: 10 μL. Semi-preparative HPLC purification was conducted on a Shimadzu HPLC System (LC-20AD, SPD-M20A) using a Luna® C18(2) column (250 × 10 mm, 5 μm, 100 Å, Phenomenex). Acetonitrile + 0.1% HCOOH and H_2O + 0.1% HCOOH was used as mobile phase. Optical rotation measurements were performed using a 0.5 dm cuvette on a JASCO P-1020 polarimeter at 25°C (unless otherwise noted).

Heterologous Expression of *pys* and pys_{PENT}

For heterologous gene expression, *Pseudomonas protegens* Pf-5 and *E. coli* HM0079 *sfp* were used as host. Suitability of the pMQ expression vector series (Shanks et al., 2006) was tested by introducing pMQ97_*gfp* into *P. protegens* Pf-5 (*via* biparental mating with *E. coli* ET12567 pUZ8002 pMQ97_*gfp*) and chemically competent *E. coli* HM0079 *sfp*. After induction with 100 mM L-arabinose (18 h), GFP was produced and fluorescent bacterial cells were visualized using a fluorescence microscope (Leika DM4500 B).

A strategy based on a gentamicin resistance ($gent^R$) selection marker was used to introduce pMQ72 shuttle vectors, encoding the full *pys* NRPS of *P. fluorescens* HKI0770 or pys_{PENT} of *P. entomophila* (sequences available at the National Center for Biotechnology Information website NCBI, WP_064118616 and WP_011533552). The corresponding pMQ72 expression vectors (Shanks et al., 2006) were constructed using the Gibson Assembly method. First, pMQ72*pys* was assembled, upon which the engineered ribosomal binding site (RBS, sequence AGGAGA) and spacer region present in pMQ97 was introduced, while keeping the XmaI site intact. The parent plasmid pMQ72 was linearized by XmaI and HindIII restriction. The NRPS gene *pys* was PCR amplified from the genomic DNA of *P. fluorescens* HKI0770 using the primer pair pMQ72pysRBS_F/R (*c.f.* Table S1). These primers include a sequence of about 20 – 25 bp that overlap with the linearized vector, and the forward primer additionally contains the RBS and spacer (the primers were designed using: http://nebuilder.neb.com). The PCR product was ligated into the pMQ72 expression vector using the standard Gibson Assembly protocol to yield expression vector pMQ72*pys*. The vector pMQ72*pys* was transformed into chemically competent *E. coli* Top10 cells *via* heat shock at 42°C. Plasmids were purified from overnight cultures (LB 15 μg/mL gentamicin) of single colonies using the QIAprep® Spin Miniprep Kit and sequenced.

From pMQ72*pys*, we generated a mutagenized plasmid, which allows for convenient expression of other *pys* homologs. We designed the expression vector to contain a cutting site 7 bp downstream of the RBS and concomitantly, we removed the *pys* ORF. To this end, pMQ72*pys* plasmid containing an RBS and a spacer region was mutagenized using the Q5® Site-Directed Mutagenesis Kit (NEB), to replace the *pys* gene (+1 bp upstream) by a short sequence containing a SalI and HindIII cutting site (GTCGACCTGCAGGCATGCAAGCT). Primers were designed using NEBaseChanger™ (setting: substitution). Following the manufacturers protocol, the vector pMQ72*rbs* was PCR amplified from pMQ72*pys* template using primers Q5SDM_pMQ72_F and Q5SDM_pMQ72_R (*c.f.* Table S1), subsequently treated with KLD enzyme mix (kinase, ligase, DpnI) and transformed into chemically competent *E. coli* Top10 cells *via* heat shock at 42°C. Plasmids were purified from overnight cultures of single colonies using the QIAprep® Spin Miniprep Kit, sequenced, and subsequently linearized by SalI and HindIII restriction.

The NRPS gene pys_{PENT} was PCR amplified from the genomic DNA of *P. entomophila* using the primer pair pMQ72pys_{PENT}_F/R (*c.f.* Table S1). These primers include a sequence of about 20 – 25 bp that overlap with the linearized vector pMQ72*rbs* (the primers were designed using: http://nebuilder.neb.com). The vector pMQ72pys_{PENT} was transformed into chemically competent *E. coli* Top10 cells *via* heat shock at 42°C. Plasmids were purified from overnight cultures (LB 15 μg/mL gentamicin) of single colonies using the QIAprep® Spin Miniprep Kit and sequenced. For heterologous expression in *E. coli*, chemically competent *E. coli* HM0079 *sfp* bearing a chromosomally installed phosphopantethein transferase (Gruenewald et al., 2004) was transformed with the respective expression vectors. For intergenic conjugation, chemically competent *E. coli* ET12567 pUZ8002 was transformed with the respective expression vectors (LB medium supplemented with 15 μg/mL gentamicin, 50 μg/mL kanamycin, and 50 μg/mL chloramphenicol). Biparental mating was performed using a standard protocol (Shanks et al., 2006). Briefly, overnight donor (*E. coli* ET12567 pUZ8002 pMQ72*pys*/pys_{PENT}) and acceptor (*P. protegens* Pf-5 or *P. entomophila*) strain cultures were mixed in a 3:1 ratio (v/v) and washed with sterile, deionized water. Mating spots (25 μL) were spotted on well-dried LB agar plates and incubated at 28°C overnight. The mating spots were then suspended in LB medium (200 μL) and plated on LB plates (100 μL, 50 μg/mL gentamicin and 100 μg/mL ampicillin). Single transformants of *P. protegens* Pf-5 pMQ72*pys* and *P. protegens* Pf-5 pMQ72pys_{PENT} were selected and used to inoculate LB medium (50 μg/mL gentamicin and 100 μg/mL ampicillin) overnight cultures, of which glycerol stocks were prepared. The generation of *P. entomophila* pMQ72pys_{PENT} was performed analogously, however the concentration of gentamicin was 75 μg/mL.

For heterologous expression, transformants were inoculated in LB medium with 100 mM L-arabinose and 15 μg/mL (*E. coli*) or 50 μg/mL (*P. protegens* Pf-5, *P. entomophila*) gentamicin, respectively. *E. coli* HM0079 *sfp* and *P. protegens* Pf-5 were cultivated as negative control. After 1 – 2 days, the cultures were extracted with ethyl acetate. The organic phase was dried over Na_2SO_4 and the solvent was removed *in vacuo*. Samples were analyzed *via* LC-MS using the standard protocol and selected ion monitoring mode for *m/z* 266 ($[M+H]^+$ pyreudione A) and *m/z* 294 ($[M+H]^+$ pyreudione B) to monitor pyreudione production.

Pys C-A Didomain Expression Vector

The genomic sequence encoding *P. fluorescens* HKI0770 pyreudione synthetase (Pys) is available at the National Center for Biotechnology Information website (NCBI, WP_064118616). An artificial ORF encoding Pys C-A didomain (979 aa, 106.95 kDa including the hexa-histidine leader sequence) was amplified from genomic DNA of *P. fluorescens* HKI0770 using the primers oDB01 and oDB02 (*c.f.* Table S1). The amplicon was assembled in the expression vector pET28a(+) (Novagen) using Gibson assembly kit (NEB). The resulting plasmid, pBK01, harbored a 2937-bp reading frame for the N-terminal hexa-histidine fusion protein (979 aa, 106.95 kDa).

Heterologous Protein Production&Purification

Escherichia coli KRX (Promega) was transformed with plasmid pBK01. An overnight pre-culture (5 mL LB, 100 mg/mL kanamycin, 37°C, 210 rpm) was grown to saturation and used to inoculate the production culture (400 mL LB, identical conditions). With an optical density of OD_{600} = 0.7 reached, gene expression was induced by supplementation of L-rhamnose to a final concentration of 0.1% (m/v) and carried out for 18 hours at 16°C. Cells were harvested by centrifugation (4°C, 3,200 × g, 30 min) and suspended in lysis buffer (50 mM $NaH_2PO_4 \cdot H_2O$, 300 mM NaCl, pH 8.0) amended with 20 mM imidazole. Disruption was carried out with a Sonopuls ultrasonic sonifier (Bandelin) and was followed by centrifugation (4°C, 17,000 × g, 20 min) for the removal of cell debris. Protein purification was performed by nickel affinity chromatography on a Protino nickel-nitrilo acetic resin (Macherey-Nagel) subjecting the sample to a stepwise imidazole gradient (20-500 mM) in lysis buffer. The purified Pys N-His_6 C-A didomain was desalted on a PD-10 desalting column (GE Healthcare) and eluted with reaction buffer (100 mM Tris, pH 7.5, 25 mM $MgCl_2$, 2.5 mM EDTA). Protein purification and concentration were verified and determined by SDS-PAGE and Bradford's assay (Bradford, 1976), respectively (*c.f.* Figure S1).

ATP-[^{32}P]pyrophosphate Exchange Assay

The ATP-[^{32}P]pyrophosphate exchange assay was performed to examine the activity and substrate predilection of the recombinant C-A didomain of Pys. The reaction mixture was composed of reaction buffer (*c.f.* Heterologous protein production&purification), 1 mM substrate, 100 nM purified enzyme, and 0.1 μM [^{32}P]pyrophosphate (50 Ci/mmol). The substrates were assayed either as pools (pool I: Gly, L-Ala, L-Val, L-Leu, L-Ile; pool II: L-Cys, L-Met, L-Ser, L-Thr, L-Pro; pool III: L-His, L-Phe, L-Tyr, L-Trp; pool IV: L-Asp, L-Asn, L-Glu, L-Gln; pool V: L-Lys, L-Arg, L-Orn), or individual pure compounds (D-proline, L/D-pipecolic acid **2**, L/D-azetidine 2-carboxylic acid **3**, pyrrole-2-carboxylic acid **5**, pyrrole-3-carboxylic acid **4**, L-hydroxyproline **6**, L-oxoproline **7**. 100 μL reactions were carried out in triplicates at 20°C. After 30 min incubation the reaction was quenched with 500 μL of an aqueous mixture of 4.6% (w/v) tetrasodium pyrophosphate and 3.5% (v/v) perchloric acid amended with 1.6% (w/v) activated charcoal. The charcoal was captured in filter paper and washed twice with quenching solution, following by suspension in 3 mL of scintillation liquid. A PerkinElmer TriCarb 2910TR scintillation counter was used for the quantification of radionuclide exchange.

LC-MS-Based Metabolomic Profiling

Potential pyreudione E (**8**) production by *Pseudomonas fluorescens* HKI0770 was analyzed after being cultured in SM/5 medium for 24 h *via* UHPLC-MS (Shimadzu). Selected ion monitoring was conducted on the calculated compound mass $[M+H]^+$ 280.2. Potential pyreudione production by *Pseudomonas entomophila* was analyzed using different media (LB, HL5, SM/5, SIH) to culture the strain. Liquid cultures (5 mL) were cultured for 1 to 3 d and extracted with 10 mL ethyl acetate. The organic phase was dried over sodium sulfate and solvents were removed using a speedvac. LC-MS samples were prepared by dissolving the crude bacterial extracts in 200 μL methanol and filtration through PTFE filter membranes (0.2 μm, Carl Roth Germany). LC-MS analysis was performed on a Kinetex® C18 column (50 × 2.1 mm, 1.7 μm, 100 Å, Phenomenex®) using a linear gradient of acetonitrile in water with 0.1% (v/v) formic acid and a flow rate of 0.7 mL/min: 10% ACN for 0.5 min, 10% to 100% ACN over 8 min, 100% ACN for 3 min. The column was equilibrated prior to each injection with 10% ACN for 2.5 min. LC-MS results were analyzed using the LabSolutions Postrun and LabSolutions Browser software (v.5.60). Potential pyreudione E (**8**) production by *Pseudomonas fluorescens* HKI0770 could be detected ($[M+H]^+$ = 280.2, t_{ret} = 6.6 min (identical mass and retention time detected for synthetic pyreudione E), whereas no pyreudione production could be detected for *P. entomophila* in any medium tested.

General Synthetic Methods

All chemicals used were reagent grade and used as supplied except where noted (Sigma Aldrich, TCI, Carl Roth, VWR, etc.). Solvents for chromatography and workup procedures were obtained from VWR (Chromanorm, HPLC grade). Reactions were performed under an argon atmosphere except where noted. Analytical thin-layer chromatography was performed on *E. Merck* silica gel 60 F_{254} plates (0.25 mm). Compounds were visualized by UV-light at 254 nm and by dipping the plates in ninhydrin solution, cerium sulfate ammonium molybdate (CAM) solution, or permanganate stain. Liquid chromatography was performed using forced flow of the indicated solvent on Normasil 60 silica gel 40-63 μm (VWR, Dresden).

Synthesis of Pyreudione E

(S)-N-Acetylpipecolic Acid 15

(*S*)-*N*-acetylpipecolic acid (**15**) was prepared according to a slightly modified procedure (Klapper et al., 2016). Briefly, 1 eq. L-pipecolic acid (**2**, 0.5 g, 3.9 mmol) and 2.5 eq. acetic anhydride were suspended in tetrahydrofuran (25 mL) and saturated aqueous sodium hydrogen carbonate solution was added until all starting material dissolved (1 mL). The reaction mixture was stirred at room temperature for 2 h, after which it was quenched by the addition of 1 M aqueous HCl. The aqueous phase was extracted with CH_2Cl_2 and the combined organic extracts were dried over Na_2SO_4. The solvent was removed *in vacuo* and the crude product purified by silica gel column chromatography (CH_2Cl_2 with MeOH, 0 to 10% v/v) to yield (S)-*N*-acetylpipecolic acid (**15**, 0.39 g, 2.3 mmol, 59%) as clear oil. All spectroscopic data were in agreement with reported values (Pizzorno and Albonico, 1977).

Weinreb Amide 16

(S)-*N*-acetyl-*N*'-methoxy-*N*'-methylpiperidine-2-carboxamide (**16**) was prepared according to a slightly modified procedure (Klapper et al., 2016; Murray et al., 1996). To a solution of (*S*)-*N*-acetylpipecolic acid (**15**, 160 mg, 0.94 mmol, 1.0 eq.) in CH_2Cl_2 (10 mL) at 0°C was added 1-ethyl-3-(3-dimethylaminopropyl) carbodiimide hydrochloride (0.54 g, 2.8 mmol, 3 eq.) and triethylamine (0.39 mL, 2.8 mmol, 3 eq.). The mixture was stirred at 0°C for 15 min after which *N*,*O*-dimethylhydroxylamine hydrochloride (0.27 g, 2.8 mmol, 3.0 eq.) was added. The reaction mixture was stirred for 1 h at 0°C and another 2 h at room temperature after which it was quenched by the addition of water. The aqueous phase was extracted with CH_2Cl_2 and the combined organic extracts were dried over Na_2SO_4. The solvent was removed *in vacuo* and the crude product purified by silica gel column chromatography (CH_2Cl_2 with MeOH 0% to 3% v/v) to yield (*S*)-*N*-acetylproline-*N'*-methoxy-*N'*-methyl amide (**16**, 0.15 g, 0.69 mmol, 74%) as clear oil. $[\alpha]_D^{24} = -7.0$ (c = 0.3 in *MeOH*); ^{1}H NMR (300 MHz, *CDCl*$_3$) δ 5.41 (bs, 1H), 3.77 (m, 4H), 3.65 (m, 1H), 3.13 (bs, 3H), 2.07 (bs, 3H), 1.95 (m, 1H), 1.34–1.77 (m, 5H); ^{13}C NMR (75 MHz, *CDCl*$_3$) δ 172.7, 171.4, 61.2, 49.0, 44.3, 31.8, 26.1, 25.1, 21.9, 19.3; HRMS (ESI+) calcd for $[C_{10}H_{18}N_2O_3+H]^+$ 215.1390, found 215.1386. NMR spectra are shown in Data S1.

Synthesis of Pyreudione E 8

Pyreudione E (2-octacyl-indolizidine-1,3-dione, **8**) was prepared according to a reported literature procedure, which was slightly modified (Klapper et al., 2016). First, the indolizidine-1,3-dione core structure (**17**) was prepared. To a solution of (S)-*N*-acetyl-*N*'-methoxy-*N*'-methylpiperidine-2-carboxamide (**16**, 69 mg, 0.32 mmol, 1 eq.) in anhydrous THF (5 mL) at –78°C was added dropwise 1.3 M lithiumhexamethyl disilazide THF solution (0.5 mL, 0.64 mmol, 2 eq.) over a period of 45 min. The reaction mixture was stirred for 3.5 h after which it was left to warm to –30°C. After another 30 min, the reaction mixture was quenched by the addition of 2 M HCl and extracted with CH_2Cl_2. The combined organic layers were dried over Na_2SO_4 and concentrated *in vacuo* to provide a crude solution of (*S*)-indolizidine-1,3-dione (**17**). Due to thermal instability, the solution was directly used for the subsequent acylation step (Klapper et al., 2016; Jeong et al., 2014). To a solution of *n*-octanoic acid (56 μL, 0.35 mmol, 1.1 eq.) in anhydrous dichloromethane (5 mL) were added EDCI (68 mg, 0.35 mmol, 1.1 eq.), DMAP (47.6 mg, 0.39 mmol, 1.2 eq.), and after 10 min crude (*S*)-indolizidine-1,3-dione (**17**, 1.0 eq.) solution (approximately 10 mL). The reaction mixture was stirred 2 hours at room temperature after which it was left for 15 h at 2°C (to complete acyl migration). The reaction mixture was quenched with saturated aqueous ammonium chloride solution. The aqueous phase was extracted with CH_2Cl_2 and the combined organic extracts were dried over Na_2SO_4. The solvent was removed *in vacuo* and the crude product purified by silica gel column chromatography (CH_2Cl_2 with methanol 0 to 5% v/v) and semi-preparative HPLC on a Luna® C18(2) column (250 × 10 mm, 5 μm, 100 Å, Phenomenex) using the following elution gradient: solvent A: H_2O + 0.1% HCOOH, solvent B: acetonitrile + 0.1% HCOOH, gradient: 75% B for 14 min, 75% to 100% B in 0.5 min, 100% B for 3 min, flow rate = 5 mL/min to obtain 22.1 mg pyreudione E (**8**) as red oil. t_R = 12.8 – 13.7 min; 25% yield; $[\alpha]_D^{25} = -1.2$ (c = 0.3 in *MeOH*); *Z:E* = 6:1; ^{1}H NMR (500 MHz, *CDCl*$_3$) δ *Z*-form 4.29 (dd, 13.4, 4.8, 1H), 3.57 (dd, 12.1, 4.1, 1H), 2.82 (m, 2H), 2.78 (m, 1H), 2.16 (m, 1H), 1.99 (m, 1H), 1.77 (m, 1H), 1.66 (p, 7.6, 2H), 1.51 (m, 1H), 1.18–1.45 (m, 10 H), 0.88 (t, 7.1, 3H); *E*-form 4.37 (dd, 13.4, 5.1, 1H), 3.73 (dd, 11.9, 4.1, 1H), 2.93 (m, 2H), 2.73 (dt, 13.0, 3.6, 1H), 2.16 (m, 1H), 1.99 (m, 1H), 1.77 (m, 1H), 1.66 (m, 2H), 1.51 (m, 1H), 1.18–1.45 (m, 10 H), 0.88 (t, 7,1, 3H); ^{13}C NMR (125 MHz, *CDCl*$_3$) δ *Z*-form 194.4, 187.9, 171.0, 101.0, 63.3, 38.5, 32.6, 31.6, 29.2, 28.9, 27.7, 26.0, 25.0, 23.3, 22.6, 14.0; *E*-form 200.6, 191.3, 164.4, 104.2, 60.3, 38.3, 32.9, 31.6, 29.3, 28.9, 27.8, 26.0, 25.0, 23.4, 22.6, 14.0; HRMS (ESI+) calcd for $[C_{16}H_{25}NO_3+H]^+$ 280.1907, found 280.1905. NMR spectra are shown in Data S1.

Feeding Experiments

Stock solutions (100 mg/mL) of amino acid substrates (L-pipecolic acid **2**, L/D-azetidine 2-carboxylic acid **3**, L-hydroxyproline **6**, and L-oxoproline **7**) as well as D-pipecolic acid (**2**) in water were sterile filtered and added to SM/5 medium for 0.1 g/L, 0.5 g/L, 1.0 g/L and 3.0 g/L final concentration of the respective amino acid. Overnight culture of *Pseudomonas fluorescens* HKI0770 was used for inoculation. After 24 h of growth at 22°C, 180 rpm, the cultures were extracted and analyzed as previously described (*c.f.* LC-MS-based metabolomic profiling). While no increase in pyreudione E (**8**, or derivatives thereof) production was observed upon addition of D-pipecolic acid, exogenous supply of 0.5 g/L L-pipecolic (**2**) acid increased production of pyreudione E (**8**) and analogues (**9** – **11**) strongly, enabling their isolation. Addition of L/D-azetidine 2-carboxylic acid (**3**) did not led to the production of respective analogues. Exogenous supply of either L-hydroxyproline (**6**) or L-oxoproline (**7**) led in both cases to the production of pyreudione I (**12**) and analogues (**13**, **14**), with 3 g/L L-hydroxyproline (**6**) in sufficient amounts for their isolation.

Isolation of Pyreudiones E – H, 8 – 11

P. fluorescens HKI0770 Δ*clp* was cultured in 3 L SM/5 medium with 0.5 g/L L-pipecolic acid (**2**). After 24 h, the culture supernatant was extracted with an equal volume of ethyl acetate and the two phases were separated. The organic phase was dried over Na_2SO_4 and the solvent was removed *in vacuo*. The crude extract was fractionated by reverse-phase column chromatography using a HyperSep™ 1g C18 column (ThermoFisher). The C18-column was washed prior use with 50 mL acetonitrile and equilibrated with 50 mL 15% acetonitrile (v/v) in water. The crude extract was dissolved in 0.5 mL MeOH and 2.85 mL water was added (final concentration of MeOH in water = 15% v/v). The solution was applied onto the conditioned C18 column. After loading, a stepwise acetonitrile-water gradient was applied to the column (15, 30, 50, 75, 100% v/v acetonitrile in water) and each fraction was collected separately. Solvents were removed using a speedvac system.

UHPLC-MS (Shimadzu System LC-30AD, SPD-M30A, LCMS-2020) analysis showed that the 75% fraction contained the highest amounts of indolizidine dione derivatives and was further purified using a semi-preparative HPLC (Shimadzu) equipped with a Luna® C18(2) column (250 × 10 mm, 5 μm, 100 Å, Phenomenex), flow rate = 5 mL/min.

The 75% acetonitrile/water fraction (45 mg) was dissolved in MeOH and purified using the following elution gradient: solvent A: H_2O + 0.1% HCOOH, solvent B: acetonitrile + 0.1% HCOOH, gradient: 80% B for 19 min, 80% to 100% B in 0.5 min, 100% B for 3 min, to yield 21.3 mg pyreudione E (**8**, t_R = 10.0 min), 3.1 mg pyreudione F (**9**, t_R = 18.1 min), 2.5 mg pyreudione G (**10**, t_R = 16.7 min), and 1.7 mg pyreudione H (**11**, t_R = 21.8min). Pyreudione G had to be repurified due to minor impurities with pyreudione D (Klapper et al., 2016). Pyreudione G was dissolved in MeOH and repurified using the following elution gradient: solvent A: H_2O + 0.1% HCOOH, solvent B: acetonitrile + 0.1% HCOOH, gradient: 62% B for 58 min, 62% to 100% B in 0.1 min, 100% B for 3 min, to yield 0.7 mg pyreudione G (**10**, t_R = 57.1 min).

Isolation of Pyreudiones I – K, 12 – 14

P. fluorescens HKI0770 Δ*clp* was cultured in 20 L SM/5 medium with 3 g/L L-4-hydroxyproline (**6**). A 200 mL pre-culture in the same medium was used for inoculation. After 20 h, the culture supernatant was extracted with an equal volume of ethyl acetate and the two phases were separated. The organic phase was dried over Na_2SO_4 and the solvent was removed *in vacuo*. The crude extract was fractionated by reverse-phase column chromatography using 15 g octadecyl-functionalized silica gel. The C18-column was washed prior use with 50 mL acetonitrile and equilibrated with 50 mL 15% acetonitrile (v/v) in water. The crude extract was dissolved in 3 mL MeOH and 16.8 mL water was added (final concentration of MeOH in water = 15% v/v). The solution was applied onto the conditioned C18 column. After loading, a stepwise acetonitrile-water gradient was applied to the column (15, 30, 50, 75, 100% v/v acetonitrile in water) and each fraction was collected separately. Solvents were removed using a speedvac system.

UHPLC-MS (Shimadzu System LC-30AD, SPD-M30A, LCMS-2020) analysis showed that the 50% fraction contained the highest amounts of hydroxylated pyrrolizidine dione derivatives and was further purified using a semi-preparative HPLC (Shimadzu) equipped with a Luna® C18(2) column (250 × 10 mm, 5 μm, 100 Å, Phenomenex), flow rate = 5 mL/min.

The 50% acetonitrile/water fraction (353 mg) was dissolved in MeOH and purified using the following elution gradient: solvent A: H_2O + 0.1% HCOOH, solvent B: acetonitrile + 0.1% HCOOH, gradient: 50% B for 14 min, 50% to 60% B in 0.5 min, 60% B for 5.5 min, 60% to 100% B in 0.5 min, 100% B for 5 min. Pyreudione I (t_{ret} = 10 – 12 min) was repurified using the following elution gradient: 48% B for 19 min, 48% to 100% B in 0.5 min, 100% B for 5 min to yield 9.6 mg pyreudione I (**12**, t_R = 16.1 min). Pyreudione J and K (t_{ret} = 19.2 – 19.8 min) were repurified using the following elution gradient: 57.5% B for 19 min, 57.5% to 100% B in 0.5 min, 100% B for 3.5 min to yield 0.8 mg pyreudione J (**13**, t_R = 19.1 min) and 1.3 mg pyreudione K (**14**, t_R = 14.2 min).

Analytical Data of Pyreudiones E – K, 8 – 14

The diastereomeric ratios were obtained from the integrals of proton 8a for pyreudione E analogues and 7a for pyreudione I analogues in the corresponding ^{1}H NMR spectra, since both diastereomers showed a well-separated peak for this single proton. For pyreudione E, the diastereomeric ratios match those of the respective synthetic compound (c.f. Synthesis of pyreudione E).

pyreudione E (**8**): *Z: E* = 6:1, $[\alpha]_D^{25} = -3.4$ (c = 0.3 in *MeOH*); HRMS (ESI+) calcd for $[C_{16}H_{25}NO_3+H]^+$ 280.1907, found 280.1906. NMR signals for both diastereomers are listed in Table S4. NMR spectra are shown in Data S1.

pyreudione F (**9**): *Z: E* = 6:1, $[\alpha]_D^{25} = -2.8$ (c = 0.3 in *MeOH*); HRMS (ESI+) calcd for $[C_{18}H_{29}NO_3+H]^+$ 308.2220, found 308.2221. NMR signals for both diastereomers are listed in Table S4. NMR spectra are shown in Data S1.

pyreudione G (**10**): *Z:E* = 9:2, $[\alpha]_D^{25} = +0.3$ (c = 0.2 in *MeOH*); HRMS (ESI+) calcd for $[C_{18}H_{27}NO_3+H]^+$ 306.2064, found 306.2069. The coupling constant between proton H2' and H3' (*J* = 15.7/15.9 Hz) suggests an *E*-configuration of the corresponding double bond (for comparison of NMR data of a related conjugated tetramic acid including a crystal structure see: Gomi et al., 1994). NMR signals for both diastereomers are listed in Table S4. NMR spectra are shown in Data S1.

pyreudione H (**11**): *Z:E* = 7:1, $[\alpha]_D^{25} = +3.5$ (c = 0.2 in *MeOH*); HRMS (ESI+) calcd for $[C_{20}H_{31}NO_3+H]^+$ 334.2377, found 334.2383. The NOESY correlation and coupling constant between proton H5' and H6' (*J* = 10.8 Hz / 10.9 Hz) suggest a *Z*-configuration of the corresponding double bond. NMR signals for both diastereomers are listed in Table S4. NMR spectra are shown in Data S1.

pyreudione I (**12**): *Z:E* = 8:3, $[\alpha]_D^{25} = -25.3$ (c = 0.2 in *MeOH*); HRMS (ESI+) calcd for $[C_{15}H_{23}NO_4+H]^+$ 282.1700, found 282.1700. NMR signals for both diastereomers are listed in Table S4. NMR spectra are shown in Data S1.

pyreudione J (**13**): *Z:E* = 3:1, $[\alpha]_D^{25} = -64.3$ (c = 0.2 in *MeOH*); HRMS (ESI+) calcd for $[C_{17}H_{25}NO_4+H]^+$ 308.1856, found 308.1855. The coupling constant between proton H2' and H3' (*J* = 15.6 Hz/15.8 Hz) suggests an *E*-configuration of the corresponding double

bond (for comparison of NMR data of a related conjugated tetramic acid including a crystal structure see: Gomi et al., 1994). NMR signals for both diastereomers are listed in Table S4. NMR spectra are shown in Data S1.

pyreudione K (**14**): *Z:E* = 3:1, $[\alpha]_D^{25} = -32.5$ (c = 0.2 in *MeOH*); HRMS (ESI+) calcd for $[C_{17}H_{25}NO_4+H]^+$ 308.1856, found 308.1858. The NOESY correlation and coupling constant between proton H3' and H4' (J = 10.6 Hz, see 2D homonuclear J-resolved ^{1}H) suggest a *Z*-configuration of the corresponding double bond. NMR signals for both diastereomers are listed in Table S4. NMR spectra are shown in Data S1.

Growth Inhibition Assay

3000 *D. discoideum* cells (AX2) were cultured in 96-well plates (Sarstedt) in 200 μL HL5 medium containing 1% DMSO (Carl Roth) and a specified amount of compound (starting from 100 μg/mL down to 0.1 μg/mL; 2-fold serial dilution) in triplicates at 22°C. The positive growth control contained only DMSO (1%). After 72 h the cell concentration was determined according to the manufacturers instruction using a CASY®Cell Counter + Analyser System (Model TT, Roche Innovatis AG) equipped with a 60 μm capillary and the evaluation cursor set to 7.5 – 17.5 μm. The viable cell concentration was plotted against the logarithmic concentration of the compound and the IC_{50} value was determined using PRISM (GraphPad, Version 5.03). The assay was repeated once and the given value is the average of both experiments.

The amoebicidal activity of pyreudione E was determined with $IC_{50} = 5.7 \pm 1.4$ μg mL^{-1}, whereas no activity ($IC_{50} > 100$ μg/mL) was found for pyreudione I.

Antimicrobial and MIC Tests

Antimicrobial activity was evaluated against *B. subtilis* 6633; *S. aureus* SG511, *E. coli* SG458, *P. aeruginosa* K799/61, *M. vaccae* 10670, *S. salmonicolor* 549, *C. albicans* C.A., and *P. notatum* JP36 by measuring the inhibition zone in mm (disc diffusion assay) according to the NCCLS (National Committee for Clinical Laboratory Standards, Clinical and Laboratory Standards Institute, 2006) and subsequent MIC testing was performed according to Wiegand et al. (2008) against *M. vaccae* 10670 and *M. aurum* SB66.

Protein BLAST

A search for homologs of the pyreudione synthetase Pys was performed using NCBI protein BLAST based on the full amino acid sequence of Pys (accession number WP_064118616, https://www.ncbi.nlm.nih.gov/). The result of this search is shown in Table S2. Only fully sequenced bacterial strains were considered. The strain available from DSMZ with the most similar *pys* homologue (*P. entomophila*) was used for further studies (heterologous expression, expression analyses).

Expression Analyses of *pys* and *pys$_{PENT}$*

For gene expression analyses, *P. fluorescens* HKI0770 and *P. entomophila* were cultured in SM/5 medium due to *P. fluorescens'* large production levels of pyreudiones in SM/5 medium. Bacterial overnight cultures of *P. fluorescens* HKI0770 and *P. entomophila* were inoculated in 5 mL SM/5 medium to OD600 = 0.1 and grown to OD600 = 1.0 (highest *pys* RNA expression levels were observed at OD600 = 1.0). RNA isolation was performed as described in the RNeasy® Mini Kit (Qiagen) manual using RNAprotect® Bacteria Reagent and 2 mL exponentially grown culture (OD600 = 1.0, ~2x10^8 cells). Residual DNA was removed with TURBO™ DNase (Thermo Fisher Scientific) and RNA was reverse-transcribed into cDNA using RevertAid Reverse Transcriptase (Thermo Fisher Scientific, 25°C 5 min, 42°C 60 min, 70°C 5 min) and Random Hexamers (Thermo Fisher Scientific). A negative control of RNA from the DNAse digestion was kept to test for complete removal of residual gDNA *via* qPCR. cDNA was purified by ethanol precipitation and resuspension, 50 ng of which were used for quantitative RT-PCR with primers amplifying *rpoD$_{HKI0770}$*/*pys$_{HKI0770}$* or *rpoD$_{PENT}$*/*pys$_{PENT}$* (*c.f.* Table S1, primers were designed using PCRTiler (Gervais et al., 2010), 400 nM final primer concentration, except for HKI0770rpoD_qPCR4_R – 800 nM, primer concentrations were optimized for equal amplification effiency) and PowerUpTM SYBR® Green Master Mix (Applied Biosystems, 95°C 2 min, then 40 times 95°C 3 sec and 62°C 30 sec, melting curve: 95°C 15 sec, 60°C 1 min, then stepwise +0.3°C to 95°C) on a StepOnePlus Real-Time PCR System (Applied Biosystems).

The fold change in expression was calculated using the $2^{-\Delta\Delta Ct}$ method (Livak and Schmittgen, 2001), comparing the gene expression of *pys* in *P. fluorescens* HKI0770 with *pys$_{PENT}$* in *P. entomophila* in three independent biological replicates. The respective *rpoD* gene was used for internal normalization. For RT-qPCR, three technical replicates were conducted for each biological replicate. The relative expression of *pys$_{PENT}$* in *P. entomophila* was set to 1.

Phylogenetic Analyses of TE Domains

Protein sequences were retrieved from public databases (for source organisms and accession numbers *c.f.* Table S3) and aligned using the MUSCLE algorithm (Edgar, 2004). In case of multi-domain proteins, only the TE domain was analyzed. Maximum likelihood trees were computed using Mega6 (Tamura et al., 2013) as follows: The best evolutionary model was determined to be the LG model (Le and Gascuel, 2008) with a gamma distribution of rates (G), invariable sites (LG + G + I + F). Therefore, this model was chosen to compute the maximum likelihood tree. A discrete Gamma distribution was used to model evolutionary rate differences among sites (5 categories (+*G*, parameter = 4.1228)). The rate variation model allowed for some sites to be evolutionarily invariable ([+*I*], 2.1950% sites). Gaps were treated as complete deletions leaving a total of 159 positions in the final dataset. The percentage of trees in which the associated taxa clustered together is shown next to the branches (bootstrap values). 100 bootstrap replicates were run to assess

consistency of branches. The TE domain of the erythromycin synthase (EryA3) was used as outgroup to root the tree. The tree is drawn to scale, with branch lengths measured in the number of substitutions per site. The tree with the highest log likelihood (-7392.1610) is shown (Figure 4). Construction of phylogenetic networks was performed with SplitsTree 4.14 (Huson, 1998) using the neighbor-net algorithm (Figure S2).

QUANTIFICATION AND STATISTICAL ANALYSIS

For growth inhibition assays, the viable cell concentration was plotted against the logarithmic concentration of the compound and the IC_{50} value was determined using PRISM (GraphPad, Version 5.03). The assay was repeated once and the given value is the average of both experiments.